This article has been accepted for publication in a future issue of this journal, but has not been fully edited. Content may change prior to final publication. Citation information: DOI 10.1109/LCOMM.2020.3028375, IEEE Communications Letters

FD-FBMC: A Solution for Multicarrier Full Duplex Cellular Systems

Kwonhue Choi, *Senior Member, IEEE*

***Abstract*—This letter reports on a critical issue with the application of OFDM to a full-duplex (FD) cellular system. With small frequency offsets of uplink signals, the downlink BER increases considerably. This is attributed to the high spectral-leakage-interference from the OFDM waveforms of geographically nearby uplink users. As an alternative, we propose applying the FBMC waveform to the same FD cellular system scenario. We calculate the precise spectral-leakage-interference for OFDM and FBMC, based on which, we set up a semi-analytic BER simulation framework. Analysis and numerical results confirm that spectral leakage interference from uplink signals is the critical performance limiting factor. Even with tiny frequency offsets among the users, the performance of FD with OFDM is severely degraded. Although the FDs with the other multicarrier waveforms having lower spectral leakage such as GFDM, UFMC, and f-OFDM overcome this issue to a certain extent, the degradations remain substantial. However, the FBMC-based FD cellular system achieves almost spectral-leakage-interference-free performance, and thus, it substantially outperforms the counterparts with other waveforms.**

***Index Terms*—cellular systems, FBMC, full duplex, OFDM.**

I. Introduction

If we employ in-band-full-duplexing of the downlink signal over uplink subbands (SBs), the downlink signal is interfered not only by its own SB uplink signal but also by the spectral leakage of uplink signals of other user equipments (UEs) at the other SBs. Thus, the downlink BER degrades because of this so-called up-to-down inter-UE inter-SB interference (U2D-IU-ISBI). The problem is that unlike the MAI of uplink signals at the BS, where the near–far effect is well managed by the power control (PC), the U2D-IU-ISBI from the geographically nearby UE(s) is very strong. In particular, for the OFDM waveform, the U2D-IU-ISBI is critical because the OFDM waveform has a large spectral leakage when the inter-carrier orthogonality is broken by the frequency offsets (FOs).

To the best of our knowledge, this critical issue—serious U2D-IU-ISBI in FD cellular systems—has never been explored in the literature. The studies in [1, 2] did not consider FOs between the downlink signal and the uplink signals of the other UEs, and therefore, only the *intra*-SB self-interference (SI) caused by FD was the major performance-limiting factor. Meanwhile, the studies in [3, 4] considered FOs in OFDM-based FD. However, they considered the FOs on the BS side [3] or in a two-node system [4]. Hence, the U2D-IU-ISBI was not considered.

This study aims to alleviate this issue. Inspired by its excellent suppression of out-of-band (OOB) power emission, we propose applying filter bank multicarrier-offset quadrature amplitude modulation (FBMC-OQAM)[1] to the FD cellular system. So far, only a few researches on combining FBMC and FD have been reported. This is mainly because the channel estimation for FBMC is more complicated than in OFDM due to the intrinsic ICI of FBMC, while the channel estimation is a crucial part for SI cancellation of FD radio. Meanwhile, the channel estimation scheme for FBMC has evolved steadily and it has reached a level achieving comparable performance to that for OFDM [5]. Therefore, it is very timely to consider integrating FD and FBMC for cellular systems in a constructive manner to exploit their merits.

The contributions of this study are listed below.

- We present a critical issue that multicarrier-based FD cellular systems undergo a new type of interference named "up-to-down inter-UE *inter*-SB interference" (U2D-IU-ISBI). In existing studies on FD cellular systems, only *intra* SB interference has been considered.
- For the OFDM-based FD cellular system (FD-OFDM) and the FMBC-based FD cellular system (FD-FDMC), we provide a compact expression for the instantaneous SINR that allows a semi-analytic BER simulation.
- For a comprehensive comparison, the BERs for FD systems with the other filter-based multicarrier waveforms, i.e., GFDM, UFMC, and f-OFDM, are evaluated by waveform-level simulation. Through intensive comparisons in various scenarios, we show that FD-FBMC is the most suitable solution to the U2D-IU-ISBI in FD cellular systems, if the SI cancellation gain is sufficiently large.

II. System model

We consider a typical single-cell FD cellular system [6–8]. The total system bandwidth is divided into multiple SBs, each of which is exclusively allocated to different UEs in the cell. The BS is equipped with an FD transceiver so that it can simultaneously transmit and receive signals on each of the SBs. For the UEs, we consider bi-directional-FD (BiFD) where each UE can simultaneously transmit and receive in the same SB as the BS [6–8]. Normally, in BiFD, each UE transmits its uplink signal overlapped in a small portion of its downlink time slot because of the asymmetry of uplink/downlink traffic. Thus, the uplink UE group is a subset of the downlink UE group.

This research was supported in part by the MSIT, Korea, under the ITRC support program (IITP-2020-2016-0-00313) supervised by the IITP, and by Basic Science Research Program through the NRF funded by the Ministry of Education(2018R1D1A3A03000837).

The author is with the Department of Information and Communication Engineering, Yeungnam University, Gyeongsan 38541, Korea (e-mail: gonew@yu.ac.kr)

[1]FBMC-OQAM is referred to as FBMC in short in this letter

This article has been accepted for publication in a future issue of this journal, but has not been fully edited. Content may change prior to final publication. Citation information: DOI 10.1109/LCOMM.2020.3028375, IEEE Communications Letters

III. Semi-analytic BER calculations of FD-OFDM and FD-FBMC

We first calculate the mean ICI powers in terms of the subcarrier distance for OFDM and FBMC. Then, based on these values, we provide computationally efficient semi-analytic BER calculations for FD-OFDM and FD-FBMC, respectively. For UFMC, f-OFDM, and GFDM, the ICI powers are determined not only by the subcarrier distance but also by the other factors because of filter distortion at the band edge or the equalization after matched filtering. Hence, for these three waveforms, we perform a waveform-level BER simulation.

A. Mean ICI power

1) OFDM case: Let ε and φ respectively denote the subcarrier spacing-normalized FO and phase offset in the received signal. Then, the signal magnitude-normalized ICI from the n-th subcarrier to the m-th subcarrier, assuming N_{FFT}-point fast Fourier transform (FFT) for multicarrier demodulation, is given as: $I_{n,m,\varepsilon} = \frac{\sin(\pi(n-m+\varepsilon))}{N_{\mathrm{FFT}}\sin(\pi(n-m+\varepsilon)/N_{\mathrm{FFT}})} e^{j\varphi}$ from which we know that the ICI does not depend on the subcarrier index but instead depends on the subcarrier index distance d (=$n-m$) and FO ε. Then, the mean ICI power is calculated as a function of d as

$$v(d) \;=\; \int_{-\Delta_f/2}^{\Delta_f/2} \left| \frac{\sin(\pi(d+x))}{N_{\mathrm{FFT}}\sin(\pi(d+x)/N_{\mathrm{FFT}})} \right|^2 f_\varepsilon(x)\mathrm{d}x \quad (1)$$

where $f_\varepsilon(x)$ is the PDF of ε distributed in the range $\left[-\Delta_f/2\ \Delta_f/2\right]$.

2) FBMC case: First, for the FBMC, the signal magnitude-normalized ICI from the lth symbol of the nth subcarrier to the pth symbol of the mth subcarrier at the matched filter output is calculated as [9]

$$\begin{aligned} I_{(n,l),(m,p),\varepsilon,\varphi} &= \Re\left\{ \int_{-\infty}^{\infty} \left(j^{n+l} h\left(t - l\frac{T}{2}\right) e^{j\left(\frac{2\pi(n+\varphi)t}{T}+\varphi\right)} \right) \right. \\ &\qquad \left. \times \left(j^{m+p} h\left(t-p\tfrac{T}{2}\right) e^{\frac{j2\pi mt}{T}} \right)^* dt \right\} \\ &= \Re\left\{ \int_{-\infty}^{\infty} j^{d+\delta} h\left(t-\delta\tfrac{T}{2}\right) h(t)\, e^{j\left(\frac{2\pi(d+\varepsilon)t}{T}+\varphi+\pi p(d+\varepsilon)\right)} dt \right\}, \quad (2) \end{aligned}$$

where $h(t)$ denotes the spectrum localization pulse with unit energy; T is the OQAM symbol duration; $\delta = l - p$; and $d = n - m$, which means that ICI is a function of the symbol index distance and the subcarrier index distance. Using the property $\Re\{X\} = |X|\cos(\angle X)$, (2) is expressed as

$$I_{(n,l),(m,p),\varepsilon,\varphi}, \;=\; \left| \int_{-\infty}^{\infty} h\left(t-\delta\frac{T}{2}\right) h(t)\, e^{j\left(\frac{2\pi(d+\varepsilon)t}{T}\right)} \mathrm{d}t \right| \cos\theta \quad (3)$$

where $\theta = \varphi + \angle\left[\int_{-\infty}^{\infty} j^{d+\delta} h\left(t-\delta\frac{T}{2}\right) h(t)\, e^{j\left(\frac{2\pi(d+\varepsilon)t}{T}+\pi p(d+\varepsilon)\right)} \mathrm{d}t \right]$. We assume that φ follows a uniform distribution over $[-\pi\ \pi]$. Then, θ follows a uniform distribution over $[-\pi\ \pi]$.

For a given d and δ, the mean ICI power averaged over θ and ε is calculated as

$$v_{d,\delta} = \frac{1}{2}\int_{-\frac{\Delta_f}{2}}^{\frac{\Delta_f}{2}} \left| \int_{-\infty}^{\infty} h\left(t-\frac{\delta T}{2}\right) h(t)\, e^{j\left(\frac{2\pi(d+x)t}{T}\right)} \mathrm{d}t, \right|^2 f_\varepsilon(x)\mathrm{d}x. \quad (4)$$

We consider the PHYDYAS pulse with $K = 4$ [10]; the pulse length of $h(t)$ is $4T(= 8\times(T/2))$. Hence, the interference from the past seven, on-time, and the next seven symbols are added assuming the sufficiently large frame size. Therefore, unlike OFDM, the mean ICI power for FBMC is calculated by adding components from multiple successive symbols as

$$v(d) \;=\; \textstyle\sum_{\delta=-7}^{7} v_{d,\delta}. \quad (5)$$

B. Signal-to-interference-plus-noise ratio

The N total system subcarriers indexed 0 to $N-1$ are divided into S SBs of size $M(=N/S)$. Each SB has N_g guard subcarriers and $N_d(=M-N_g)$ data sub-carriers. Let $n_{k,i}$ denote the subcarrier index of the ith data subcarrier of the kth SB in the total subcarrier axis ranging from 0 to $N-1$. Then, $n_{k,i} = (k-1)M + i$.

If we denote $\gamma_{k,i}$ as the downlink post-detection signal-to-interference-plus-noise ratio (SINR) of the ith data subcarrier of the kth SB (=$n_{k,i}$th subcarrier), it is formulated as

$$\gamma_{k,i} = \frac{\alpha_k^{(d)} E_s}{N_0 + 2T\sum_{j\in\mathbf{s}} \rho_{(j,k),i}} \quad (6)$$

where E_s is the data symbol energy, $\alpha_k^{(d)}$ is the fading gain, $N_0/2$ is the background noise density, and $\mathbf{s}$ denotes the index set of K_u SBs.

The term $\rho_{(j,k),i}$ denotes the total ICI power from the uplink signal in the jth SB to the downlink signal at the ith data subcarrier of the kth SB (= $n_{k,i}$th subcarrier) and it is given as

$$\rho_{(j,k),i} \;=\; \textstyle\sum_{l=0}^{N_d-1} g_{(j,k)} \times p_j \times v(n_{j,l} - n_{k,i}) \quad (7)$$

where the mean ICI power function $v(x)$ is equal to (1) for OFDM, and it is equal to (5) for FBMC. The variable p_j in (7) denotes the uplink subcarrier transmit power of the jth SB, and it is set such that the received SNR in the BS is equal to its target value, denoted by γ_o. Hence, p_j is set as

$$p_j \;=\; (\gamma_0 N_0/T)\left(L_j^{\mathrm{B-U}}\right)^{-1}, \quad (8)$$

where $L_j^{\mathrm{B-U}}$ is the overall channel link gain by path loss and shadow fading between the BS and uplink UE at the jth SB. The variable $g_{(j,k)}$ in (7) denotes the channel gain from the uplink UE allocated to the jth SB to the downlink UE allocated to the kth SB.

If $j \neq k$, $\rho_{(j,k),i}$ is U2D-IU-ISBI power, in this case, $g_{(j,k)}$ is set as

$$g_{(j,k)} \;=\; \alpha_{(j,k)} L_{(j,k)}^{\mathrm{U-U}}, \quad (9)$$

where $\alpha_{(j,k)}$ is the fading gain, and $L_{(j,k)}^{\mathrm{U-U}}$ is the overall channel link gain by path loss and shadow fading between the uplink UE at the jth SB and the downlink UE at the kth SB.

Substituting (9) and (8) into (7), $\rho_{(j,k),i}$ is given as

$$\rho_{(j,k),i} = (\gamma_0 N_0 \alpha_{(j,k)}/T)\left(\frac{L_{(j,k)}^{\mathrm{U-U}}}{L_j^{\mathrm{B-U}}}\right) \sum_{l=0}^{N_d-1} v(n_{j,l} - n_{k,i}). \quad (10)$$

Note that there is a scaling term $\left(L_{(j,k)}^{\mathrm{U-U}}/L_j^{\mathrm{B-U}}\right)$ in (10). This scaling term varies widely, as it is a ratio whose numerator and

This article has been accepted for publication in a future issue of this journal, but has not been fully edited. Content may change prior to final publication. Citation information: DOI 10.1109/LCOMM.2020.3028375, IEEE Communications Letters

denominator vary widely and independently; thus, it significantly amplifies the ICI power sum $\sum_{l=0}^{N_d-1} v(n_{j,l} - n_{k,i})$ when $\left(L_{(j,k)}^{\text{U-U}}/L_j^{\text{B-U}}\right)$ is very large, for instance, when the interfering uplink UE is far from the BS and close to the desired downlink UE. This scenario leads to a substantial increase in the overall interference to the desired downlink UE.

If $j = k$ for BiFD, $\rho_{(k,k),i}$ is the residual SI (RSI) power, and in this case, $g_{(k,k)}$ is the equivalent channel gain of the RSI, which is given as $g_{(k,k)} = 1/\beta$, where β denotes the total SI cancellation gain (higher is better) including passive (such as antenna separation), analog, and digital cancellations. If $j = k$ for TNFD, $g_{(k,k)}$ is expressed as in (9); however, in this case, $\rho_{(k,k),i}$ implies U2D-IU-*intra*-SBI.

If p_j in (8) is set too high in the case of the low channel link gain, it induces a high RSI despite the SI cancellation for BiFD, probably causing an unacceptable BER increase. Hence, in such a case, it is beneficial to pause one of the downlink or uplink signals. Specifically, if the mean RSI-to-noise ratio (RSINR) calculated as $\frac{2Tp_j}{\beta N_0}$ is larger than a predetermined threshold denoted by RSINR_0, the downlink signal is paused until the uplink transmission finishes.

C. BER

We use a semi-analytic approach to calculate the BER. Using the derived expression for SINR in (6), the average BER of the $n_{k,i}$th subcarrier can be obtained as

$$\text{BER}_{k,i} = \text{E}_{\left\{\alpha_k^{(d)}, \bar{\mathbf{g}}, \bar{\mathbf{p}}\right\}} \left[p_\text{b}(\gamma_{k,i})\right] \quad (11)$$

where $p_\text{b}(x)$ is the instantaneous BER; for instance, $p_\text{b}(x) = 0.5\text{erfc}(\sqrt{x})$ for binary phase-shift keying (BPSK), and $p_\text{b}(x) = 0.5\text{erfc}(\sqrt{x/2})$ for quadrature phase shift keying (QPSK)[2]. The vectors $\bar{\mathbf{g}}$ and $\bar{\mathbf{p}}$ denote a set of $g_{(j,k)}$ for $\forall j \in \mathbf{s}$ and a set of p_j for $\forall j \in \mathbf{s}$, respectively. As the last step, we need to average $\text{BER}_{k,i}$ over the entire data subcarrier of the entire downlink SBs.

IV. Numerical results

We consider a small-cell network, which is suitable for FD because of its low transmit power and low mobility. The simulation parameters are commonly set as: cell radius = 50 m, subcarrier spacing $1/T$= 15 kHz, N = 256, S = 16, and $N_0/2$= -174 dBm/Hz, with QPSK modulation. The UEs are uniformly distributed in the cell. Considering the geometrical and environmental differences between the BS–UE and UE–UE links, the channel propagation gains for BS–UE link ($\alpha_k^{(d)}$, $L_j^{\text{B-U}}$), and those for the BS–UE link ($\alpha_{(j,k)}$, $L_j^{\text{U-U}}$) are generated separately using the measurement-based small-cell models in Tables 6.2-1 and 6.3-1 in [14].

As for the waveform-specific parameters other than the common system parameters mentioned above, we adopt the settings in [10], [11], [12], and [13] for FBMC, f-OFDM, UFMC and GFDM, respectively, which are widely used in the related literature.

[2]This error function assumes that the interference term in (6) is Gaussian. For FBMC, this assumption may not be valid, since the number of subcarriers contributing to the interference is insufficient to invoke the Central Limit Theorem. However the waveform-level simulation results in Fig. 2 show that the calculation is nevertheless accurate.

A. Case with identical SI cancellation among the waveforms

Fig. 1 shows BERs versus Δ_f for various situations when multiple FD UEs are active in a cell. The first sub-figure shows the case when the maximum number of FD UEs in a cell is active, i.e., $K_d = S(= 16)$, $K_u = S(= 16)$; one guard subcarrier per SB was inserted ($N_g = 1$). The BERs of the FD-OFDM abruptly increase even though Δ_f increases slightly; this is attributed to the U2D-IU-ISBI of FD-OFDM becoming serious for the downlink signals, which agrees with the conjecture based on the analysis of (10), presented in the previous section. FD-GFDM and FD-UFMC perform better than FD-OFDM due to the lower OOB emissions; however, the BERs remain considerably larger than the noise-only level, which is about 2 $\times 10^{-4}$. The FD-f-OFDM undergoes significant BER degradation even with Δ_f=0. This is attributed to the f-OFDM requiring a non-negligible excess bandwidth (BW) (1.5 subcarrier spacing) to avoid filtering out the main side-lobes of the band edge subcarriers. It is remarkable that the FD-FBMC proposed for the cellular system in this study achieves an almost noise-only BER performance. This confirms that FBMC has negligible U2D-IU-ISBI because of its excellent OOB suppression compared to the other waveforms.

A comparison of the results with β= 80 dB in the second sub-figure of Fig. 1 with that for β = 120 dB in the first sub-figure indicates that the BER for no FO (Δ_f = 0) is shifted upwards because of non-negligible RSI; however, the overall trends according to the waveforms remain the same. The third sub-figure in Fig. 1 shows the case when the number of active FD UEs is 4 (K_u = 4), i.e., only 4 out of S(= 16) SBs are active for uplink signal transmission. The SBs for the active FD-UEs are randomly allocated from the total S(= 16) SBs. Although the BERs are lowered substantially by the reduced number of uplink signals causing the reduced U2D-IU-ISBI, the BER gaps between the FD systems with different waveforms remain substantial. This means that even for low uplink traffic, the significant BER degradation of the downlink UEs with SBs that are next to the SB(s) of uplink UEs dominates the average downlink BER of the FD cellular system.

A simple and explicit approach to reduce U2D-IU-ISBI is to insert more guard subcarriers. The fourth sub-figure in Fig. 1 shows the results when N_g is increased to 3. Note that the BERs of the FD-OFDM and FD-UFMC, even with N_g= 3, are slightly lower than those with N_g=1 in the first sub-figure. However, for FD-GFDM and FD-f-OFDM, increasing the number of guard subcarriers is very effective in reducing the BER. This is because GFDM and f-OFDM have sharper band edges than UFMC because of their longer pulse length compared to that for UFMC. However, inserting guard subcarriers results in spectral efficiency loss. For instance, increasing N_g to 3 results in 13.3 % loss compared to the case of N_g=1 with M=16. Moreover, the BERs are still larger than that of FD-FBMC with N_g=1. A more active solution to reduce U2D-IU-ISBI is using a tighter spectrum-shaping filter; however, this approach requires larger filter transients or larger CP lengths, which decrease the spectral efficiency. In addition, a smaller excess BW for f-OFDM results in a higher distortion to the band edge subcarrier and thus a worse BER for the case

This article has been accepted for publication in a future issue of this journal, but has not been fully edited. Content may change prior to final publication. Citation information: DOI 10.1109/LCOMM.2020.3028375, IEEE Communications Letters

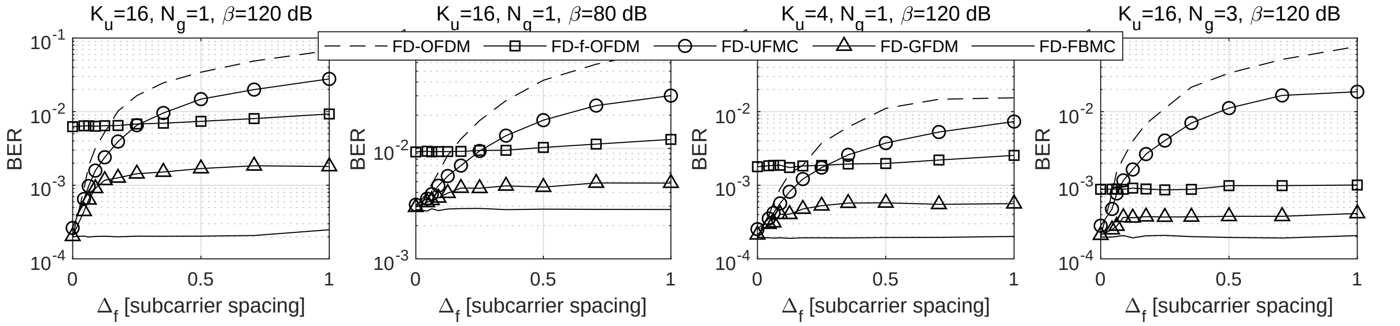

Fig. 1: BER versus Δ_f, K_d=16, E_s/N_0=11 dB, $\gamma_0 = E_s/N_0$, and RSINR_0=0 dB.

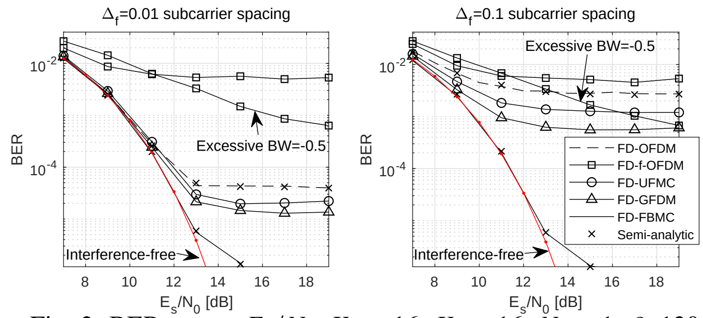

Fig. 2: BER versus E_s/N_0, K_d = 16, K_u = 16, N_g = 1, β=120 dB, $\gamma_0 = E_s/N_0$, and RSINR_0 = 0 dB.

of no U2D-IU-ISBI.

Even with a tight uplink synchronization in cellular systems, the nonzero FOs of uplink UEs are inevitable. The left side sub-figure in Fig. 2 shows the BER curves when Δ_f=0.01, as an example of tiny FOs among the uplink signals. For a neat presentation, we put the legend box only in the right side sub-figure. The semi-analytic simulation results obtained by (11) are included with a mark '×' for FD-OFDM and FD-FBMC, and they confirm that the proposed semi-analytic BER calculation achieves considerably accurate results. The interference term was assumed to be Gaussian in the semi-analytic simulation. Hence, it is also confirmed that the Gaussian assumption works well for FD-FBMC as well as for FD-OFDM. There are small BER gaps among the FD systems with different waveforms except f-OFDM in the low SNR region. However, as the SNR increases, the BER gaps between FD-FBMC and the other waveform-based FD systems become significant. For the case with Δ_f=0.1 in the right side sub-figure, the BERs of the FD systems with OFDM, GFDM, and UFMC significantly degrade over the entire SNR region, and their BERs saturate to unacceptable levels in the high SNR region, whereas FD-FBMC undergoes almost no degradation. Note that a tight excess BW for f-OFDM (excess BW = -0.5 subcarrier spacing in the figures) degrades the BER in the low SNR region where the noise power is larger than U2D-IU-ISBI power; however, in the U2D-IU-ISBI dominant region (high SNR region with non-negligible FOs), it can be a solution to catch up with the performances of FD systems with OFDM, UFDM, and GFDM.

B. Case with the worst (maximum) SI cancellation penalty for FBMC

The SI at the input to digital SI cancellation stage suffers its own ICI, which degrades SI cancellation performance. In order to analyse how the ICI of SI affects the FD systems with different waveforms, we consider the oscillator phase noise (PN) that is the main limiting factor of SI cancellation [15, 16].

Denote the PNs at transmitter (TX) and receiver (RX) oscillators as $\theta_T(t)$ and $\theta_R(t)$ and denote the transmission delay t_d, then, a phase rotation process $e^{j(\theta_T(t-t_d)-\theta_R(t))}$ is multiplied to the input to digital SI cancellation stage. The PN $\theta_X(t)$, $X \in \{T, R\}$ is modelled as Winner process where $\theta_X(t)-\theta_X(t-\tau)$ is normally distributed with variance $4\pi f_{3dB}\tau$ and f_{3dB} is the 3dB BW of the PN Lorentzian spectrum. For the case of two separate oscillators (Two Sep. Osc.'s) for TX and RX, $\theta_T(t)$ and $\theta_R(t)$ are independent each other, and for the case of one common oscillator (One Com. Osc.) for TX and RX, $\theta_T(t)$ is equal to $\theta_R(t)$. Let Y_n denote the demodulated output of the nth subcarrier of SI prior to digital SI cancellation. Then, with the PNs $\theta_T(t)$ and $\theta_R(t)$, Y_n is given as: $Y_n = Y_{n,0} + Y_{n,ICI} + w_n$ where $Y_{n,0}$ $Y_{n,ICI}$ and w_n denote the data symbol term of the nth subcarrier, PN-induced ICI term to the nth subcarrier, and noise term, respectively. The ICI term increases SI channel estimation error which degrades SI cancellation gain (β). Therefore, we can assess differences of β among the waveforms by comparing the ICI power among the waveforms, although we did not implement the digital SI cancellation algorithm as it is out of scope of this study. To this end, we added PN effect in the waveform-level simulation and calculated the mean power of normalized ICI, p_{ICI} given as: $p_{ICI} = \text{E}\left[\frac{1}{N_d}\sum_n \left|\frac{Y_{n,ICI}}{Y_{n,0}}\right|^2\right]$ for each of the waveforms, and the results are shown in the left sub-figure of Fig. 3 as a function of subcarrier spacing-normalized PN BW δ_f equal to $f_{3dB}T$. It is found that there are considerable differences in ICI power among the waveforms, and FBMC has higher ICI power than OFDM, GFDM and UFMC which have the similar ICI powers. This is because unlike U2D-IU-ISBI which comes from the other SBs, the ICI of SI mainly comes from the very next subcarriers in the same SB, which is severe for FBMC due to its intrinsic ICI.

Note that the slope (in dB scale) of ICI power versus δ_f in Fig. 3 for OFDM is approximately equal to the maximally decreasing slope (in dB scale) of SI cancellation gain (β) versus δ_f in Figure 2 in [15] (or increasing slope in Figure 5 in [16]). From this observation, we can set up a relation that in

This article has been accepted for publication in a future issue of this journal, but has not been fully edited. Content may change prior to final publication. Citation information: DOI 10.1109/LCOMM.2020.3028375, IEEE Communications Letters

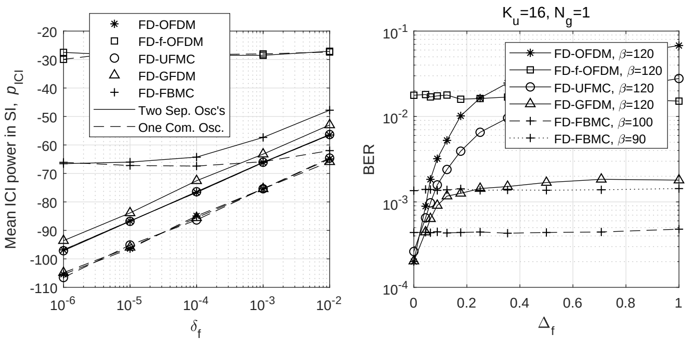

Fig. 3: Left sub-figure: mean ICI power versus PN bandwidth, t_d=$T/16$ for One Com. Osc., Right sub-figure: BERs versus E_s/N_0 with the same parameters as in the first sub-figure in Fig. 1 but with reduced βs for FBMC.

dB scale, the maximum decreasing slope of β versus ICI power is equal to 1 dB/dB, i.e., the maximum reduction of β by the ICI power increase is as large as the increase of ICI power. For instance, for two separate oscillator case with $\delta_f = 10^{-5}$ in the left sub-figure of Fig. 3, the ICI power of FBMC is about 20 dB higher than those of OFDM, UFMC and GDFM and thus, the FBMC has lower β than those of OFDM, UFMC and GDFM with 20 dB difference for the worst case. It is shown in the right sub-figure of Fig. 3 that the BER of FBMC with 20 dB-lower β (i.e., $\beta = 100$) is slightly larger than those of OFDM/UFMC/GFDM with $\beta = 120$ for small Δ_fs, whereas the FBMC still achieves substantially lower BERs than the other waveforms for Δ_f larger than about 0.05. Similarly for one common oscillator case with $\delta_f = 10^{-5}$ and $t_d = T/16$, the FBMC has lower β than those of OFDM/UFMC/GFDM with 30 dB difference for the worst case. The BER of FBMC with 30 dB-lower β (i.e., $\beta = 90$) is larger than those of GFDM/UFMC/OFDM with $\beta = 120$ for Δ_f smaller than 0.25, 0.08 and 0.06, respectively. However, as Δ_f increases, FBMC still substantially outperforms OFDM and UFMC.

As these results are based on the maximum slope of β versus δ_f in Figure 2 of [15], we can expect the less reduction of β against ICI power increase than 1 dB/dB. Moreover, it is shown in the left sub-figure of Fig. 3 that as δ_f increases, the ICI power differences between FBMC and the other waveforms decrease. Especially for the case with one common oscillator, the differences become negligible. Accordingly, the BER gaps between FBMC and the other waveforms are recovered to those observed in Section IV-A.

It is observed from Figure 2 of [15] that β saturates in the range of $\delta_f < 10^{-5}$. Hence, although ICI power difference between FBMC and the other waveforms further increase in the range of $\delta_f < 10^{-5}$, it would not make further differences of β between FBMC and the other waveforms.

V. Conclusions

We discovered that in OFDM-based FD cellular systems, the downlink BER severely degrades because of U2D-IU-ISBI. As an alternative, we proposed applying FBMC to an FD cellular system. For a comprehensive comparison, the BERs for FD systems with GFDM, UFMC, and f-OFDM, were also evaluated. Through intensive comparisons under various situations, we show that FD-FBMC is the most suitable solution to the issue of U2D-IU-ISBI in FD cellular systems, if the SI cancellation gain is sufficiently large.

References

[1] A. C. Cirik, K. Rikkinen, and M. Latva-aho, "Joint subcarrier and power allocation for sum-rate maximization in ofdma full-duplex systems," in *2015 IEEE 81st Vehicular Technology Conference (VTC Spring)*, 2015, pp. 1-5.

[2] C. Nam, C. Joo, and S. Bahk, "Radio resource allocation with inter-node interference in full-duplex OFDMA networks," in *Proc. IEEE ICC*, 2015, pp. 3885-3890.

[3] S. Shaboyan, *et al.*, "Frequency and timing synchronization for in-band full-duplex OFDM system," *IEEE GLOBECOM*, Singapore, Dec. 2017, pp. 1-7.

[4] Y. Liu, X. Zhu, E. G. Lim, Y. Jiang, and Y. Huang, "Fast iterative semi-blind receiver for URLLC in short-frame full-duplex systems with CFO," *IEEE J. Sel. Areas Commun.*, vol. 37, pp. 839-853, Apr. 2019.

[5] C. Lele, P. Siohan and R. Legouable, "2dB Better Than CP-OFDM with OFDM/OQAM for Preamble-Based Channel Estimation," *IEEE ICC 2008*, pp. 1302-1306, May 2008.

[6] C. Nam, C. Joo, and S. Bahk, "Joint subcarrier assignment and power allocation in full-duplex OFDMA networks," *IEEE Trans. Wireless Commun.*, vol. 14, no. 6, pp. 3108-3119, Jun. 2015.

[7] T. T. Tran, V. N. Ha, L. B. Le, and A. Girard, "Dynamic resource allocation for full-duplex ofdma wireless cellular networks," in *IEEE VTC*, Sept 2016, pp.1-5.

[8] P. Tehrani, F. Lahouti, and M. Zorzi, "Resource allocation in OFDMA networks with half-duplex and imperfect full-duplex users," *IEEE ICC*, May 2016, pp. 1-6.

[9] D. Na and K. Choi, "Low PAPR FBMC," *IEEE Trans. Wireless Commun.*, vol. 17, no. 1, pp. 182-193, Jan. 2018.

[10] M. Bellanger, *et al.*, FBMC Physical Layer: A Primer. PHYDYAS, Jan. 2010.

[11] https://www.mathworks.com/help/comm/examples/f-ofdm-vs-ofdm-modulation.html

[12] https://www.mathworks.com/help/comm/examples/ufmc-vs-ofdm-modulation.html

[13] https://github.com/vodafone-chair/gfdm-lib-matlab

[14] "Further enhancements to LTE time division duplex (TDD) for downlink-uplink (DL-UL) interference management and traffic adaptation," in *3GPP TR 36.828 v11.0.0*, Jun. 2012.

[15] X. Quan,*et al.*, "Impacts of phase noise on digital self-interference cancellation in full-duplex communications," *IEEE Trans. Signal Process.*, vol. 65, no. 7, pp. 1881-1893, Apr. 2017.

[16] V. Syrjala, *et al.*, "Analysis of Oscillator Phase-Noise Effects on Self-Interference Cancellation in Full-Duplex OFDM Radio Transceivers", *IEEE Trans. Wirel. Commun.*, vol. 13, no. 6, pp. 2977-2990, June 2014.